Power system stability with parallel active filter ensuring compensation of capacitive reactive power of a resonant LC circuit

T. PLATEK*

Institute of Control and Industrial Electronics, Warsaw University of Technology, 75 Koszykowa St., 00-662 Warsaw, Poland

Abstract. This paper presents an analysis allowing for the determination of the differential equation describing the circuit of the active filter inverter output current control with an additional measurement of input voltage. The resulting equation allows to determine the conditions that ensure stable operation of the filter with the load in form of a resonant LC circuit. Analysis results were confirmed by computer simulation and experimental studies of commercial active filter.

Key words: parallel active filter, passive filter, system stability analysis.

1. Introduction

Recently, because of increasing demand in respect to power quality and smart Grids development [1], the importance of active filters has been continuously growing.

This article is a continuation of the discussion presented in [2] concerning the stability of a power system with an active filter, compensating capacitive reactive power load containing the elements of a purely capacitive nature (cables, capacitors). The analysis presented in this article relates to the power system with a hybrid filter [3], in which the active filter besides reduction of deformation power is supposed to compensate the phase shift reactive power introduced by a passive *LC* filter capacitor. In the case of an unstable operation each active filter should be automatically disconnected from the grid, but in such systems as hybrid filters, a stable operation must be ensured.

One solution to ensure the stability of the hybrid filter is to program an active filter operation [4–6] so that it does not compensate the *LC* circuit resonant frequency components. Another solution to the problem of stability of a system with the *LC* resonant branch is to separate the component proportional to the current of the resonance branch from the reference signal for the output current of an active filter, but this means no compensation of a component of the displacement reactive power absorbed by the resonant circuit.

This article describes another solution for a stable power supply system with a hybrid filter. It involves feeding to the active filter current controller input the signal proportional to the voltage measured at the terminals of the filter on the AC voltage signal, its derivative and the derivative of the signal of the load current.

2. The equations describing filter output current control loop

Figure 1 shows schematic diagram of the analyzed power system with hybrid filters, whereas Fig. 2 shows the equivalent circuit of an active filter control system, together with a feedback system – which ensures the stability of the filter with capacitive load. The active filter is based on the *FLC* type three-level voltage inverter with variable potential capacitors.

The filter compensates higher harmonics in current drawn by nonlinear load (6D converter) and capacitive reactive power generated of the passive *LpCp* filter.

The control system shown in Fig. 2. with the voltage regulator in the DC circuit implements the algorithm described in the literature [7]. Supervisory u_{DC} voltage regulator stabilizes it to the set value, proportional to U_{DC}^*. Unit signals u_{1ref}, u_{2ref}, u_{3ref} are in phase with the power supply voltages u_{s1}, u_{s2}, u_{s3} which causes the controller output signal to set amplitude and phase (0 or π rad) of the sine component of inverter output currents. Such a control ensures discharging or charging C_{DC} capacitor in transient conditions, associated with the change of an active power consumed by the load. The active filter operates in an open system, which means that it uses the signals of the load currents. These controls provide a very short reproduction time of setpoint signals (u_{i1ref}, u_{i2ref}, u_{i3ref}) setting the filter inverter output current at changes of the active power of the receiver. This is tantamount to a short voltage regulation time in the DC circuit of an active filter.

Systems of band-stop filters with ω_s pulsation shunted by $S1$, $S2$, $S3$ switches allow for programming two modes of a filter operation: with compensation of passive displacement power ($S1$, $S2$, $S3$ conducting) or without compensation of passive displacement power ($S1$, $S2$, $S3$ open).

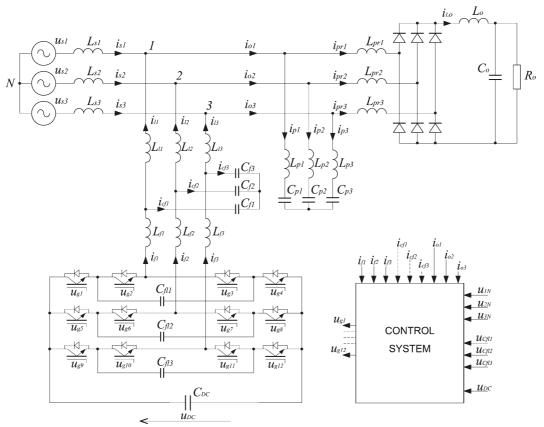*e-mail: platek@isep.pw.edu.pl

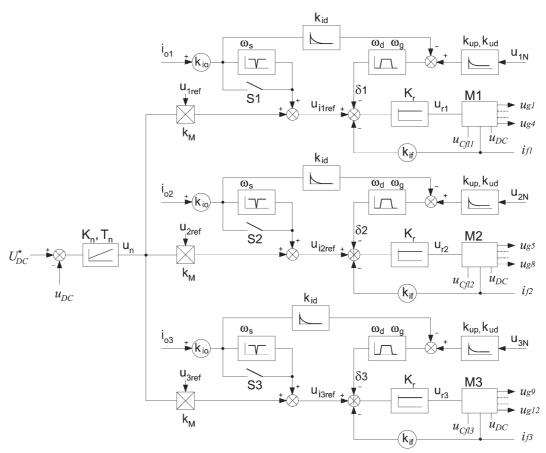Fig. 1. Schematic diagram of the analyzed system with active filter

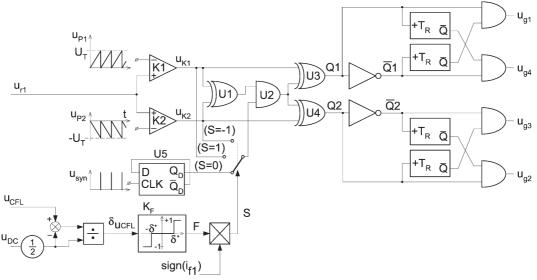Fig. 2. Equivalent circuit of active filter control system

Fig. 3. Block diagram of $M1$ modulator

The proposed method of stabilizing operation of the power system allows maintaining of these dynamic properties of the filter. The input of current regulator takes the feedback signals proportional to the inverter output currents, signals proportional to the voltage measured at the terminals on the AC side of the inverter, their derivatives, and the signals proportional to the derivative of the load current. The task of the bandpass filter with lower pulsation ω_d (larger than the pulsation ω_s of phase voltages) and the upper ω_g pulsation (lower than the resonant circuit pulsation of $L_f C_f$ circuit) placed at the output of sum of Proportional-Derivative Block (k_{up}, k_{ud}) output and Derivative Block (k_{id}) output is to eliminate the impact of components outside its frequency response on the filter operation. As follows from further consideration, additional feedbacks with k_{up}, k_{ud}, k_{id} coefficients can optimize the coefficients values of the differential equation describing the power system with active filter.

Figure 3 shows a block diagram of three level inverter modulator with an additional u_{CFL} leveling voltage regulation and stabilization [8]. Each of the modulators $M1$, $M2$, $M3$ consists of two comparators ($K1$, $K2$) and logic system ($U1 \div U5$). The modulator uses two synchronized by u_{syn} sawtooth waveform carrier signal u_{P1}, u_{P2} of different polarities, fed to the inverting inputs of comparators. This solution improves the shape of the formed output current of the inverter. The control system forces the inverter operating states that are described by a pair of signals $Q2$, $Q1$. K_F nonlinear system, whose output signal F indicates the exceeded limit value of error δ_{UCFL} and taking additionally into account the current polarity i_{f1}, decides on the state of the modulator output ($Q2$, $Q1$) for the middle level.

Inverter operation is synchronized by u_{syn} impulses, whose front edges determine the moments of reading in the u_r control value, in order to determine the pair of voltage at its output and the choice of operation mode. The falling edges of the u_{K1} or u_{K2} signal correspond to the choice of another operation mode. Sampling frequency is two times

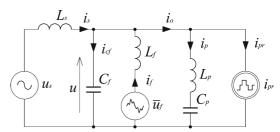higher than the average switching frequency of inverter transistors.

Fig. 4. Equivalent circuit of one phase of the supply system with hybrid filter

The schematic diagram of the supply system with active filter shown in Fig. 1 can be, by omitting L_{l1}, L_{l2}, L_{l3} inductances (these inductance are lower by an order than the corresponding inductance L_{f1}, L_{f2}, L_{f3}), simplified for each phase to the diagram shown in Figure4. The L_s, C_f, L_f, L_p, C_p inductances and capacitances of one-phase system are equal to L_{s1}, L_{s2}, L_{s3}, C_{f1}, C_{f2}, C_{f3}, L_{f1}, L_{f2}, L_{f3}, L_{p1}, L_{p2}, L_{p3}, C_{p1}, C_{p2}, C_{p3} inductances and capacitances of the three-phase system, respectively.

Based on the equivalent diagrams shown in Figs. 1–4 for any phase one can write:

$$\overline{u}_f = \left(u_{iref} - k_{if}i_f - k_{up}u - k_{ud}\frac{du}{dt} + k_{io}k_{id}\frac{di_o}{dt} \right) K_R,$$

$$(1)$$

K_R is equivalent gain of the proportional controller in the circuit,

$$K_R = \frac{K_r u_{DC}(1 - t_{dead}f_{syn})}{2U_T},$$

$$(2)$$

where f_{syn} is the frequency of the auxiliary sawtooth voltage with a maximum value of U_T, $\overline{u}_f$ is the average value of phase inverter output voltage for $T_{syn} = 1/f_{syn}$ period of output phase inverter voltage, t_{dead} is the minimum time of simultaneous switch on of transistors of each pair forming a switching circuit in the inverter branches.

The introduction of a third feedback signal to the summing node of current controller, proportional to the derivative of the load current by a factor k_{id}, is to ensure the ability to obtain appropriate values of the coefficients of the characteristic equation of the expected fourth order. If we assume that:

$$\overline{u}_f = L_f \frac{di_f}{dt} + u. \tag{3}$$

Then (1) can be written in new form (4):

$$k_{if} i_f = u_{iref} - k_{up} u - k_{ud} \frac{du}{dt}$$
$$+ k_{io} k_{id} \frac{di_o}{dt} - \frac{1}{K_R} \left(L_f \frac{di_f}{dt} + u \right). \tag{4}$$

In these relations the following sum of two components constitutes the u_{iref} reference signal for i_f:

$$u_{iref} = u_n k_M u_{ref} + k_{io} i_o. \tag{5}$$

Considering (5) in relation (4) we obtain:

$$k_{if} i_f - u_n k_M u_{ref} - k_{io} i_o + k_{up} u + k_{ud} \frac{du}{dt}$$
$$- k_{io} k_{id} \frac{di_o}{dt} + \frac{1}{K_R} L_f \frac{di_f}{dt} + \frac{1}{K_R} u = 0. \tag{6}$$

After differentiation of both side of Eq. (6) with reference to time we obtain:

$$k_{if} \frac{di_f}{dt} - k_M \frac{d}{dt}(u_n * u_{ref}) - k_{io} \frac{di_o}{dt} + k_{up} \frac{du}{dt}$$
$$+ k_{ud} \frac{d^2 u}{dt^2} - k_{io} k_{id} \frac{d^2 i_o}{dt^2} + \frac{1}{K_R} L_f \frac{d^2 i_f}{dt^2} + \frac{1}{K_R} \frac{du}{dt} = 0. \tag{7}$$

Based on diagram for one phase (Fig. 4) we can write the equation for currents:

$$i_s = i_{cf} - i_f + i_p + i_{pr}. \tag{8}$$

Particular currents are described by the following relations:

$$i_{cf} = C_f \frac{du}{dt}, \tag{9}$$

$$i_s = \frac{1}{L_s} \int_{t_o}^{t} (u_s - u) d\tau + i_s(t_o), \tag{10}$$

$$u = L_p \frac{di_p}{dt} + \frac{1}{C_p} \int_{t_o}^{t} i_p d\tau + u_{cp}(t_o), \tag{11}$$

$$i_o = i_p + i_{pr}. \tag{12}$$

From Eqs. (8) and (9) we can determine the first and second derivative of i_f current:

$$\frac{di_f}{dt} = C_f \frac{d^2 u}{dt^2} + \frac{di_p}{dt} + \frac{di_{pr}}{dt} - \frac{di_s}{dt}, \tag{13}$$

$$\frac{d^2 i_f}{dt^2} = C_f \frac{d^3 u}{dt^3} + \frac{d^2 i_p}{dt^2} + \frac{d^2 i_{pr}}{dt^2} - \frac{d^2 i_s}{dt^2}. \tag{14}$$

After substituting (10)–(14) to (7) we obtain the differential equation, describing – with these principles – active filter operation with the adopted control:

$$\frac{L_f C_f L_p}{K_R} \frac{d^5 i_p}{dt^5}$$
$$+ L_p (k_{if} C_f + k_{ud}) \frac{d^4 i_p}{dt^4}$$
$$+ \frac{K_R \left(k_{up} - \frac{k_{io} k_{id}}{L_p} \right) + 1 + \frac{L_f}{L_s} + \frac{L_f}{L_p} \left(1 + \frac{C_f}{C_p} \right)}{\frac{K_R}{L_p}} \frac{d^3 i_p}{dt^3}$$
$$+ \left[k_{if} \left(1 + \frac{L_p}{L_s} + \frac{C_f}{C_p} \right) - k_{io} + \frac{k_{ud}}{C_p} \right] \frac{d^2 i_p}{dt^2}$$
$$+ \frac{1}{K_R C_p} \left(k_{up} K_R + 1 + \frac{L_f}{L_s} \right) \frac{di_p}{dt}$$
$$+ \frac{k_{if}}{C_p L_s} i_p$$
$$= \frac{k_{if}}{L_s} \frac{du_s}{dt} + \frac{L_f}{K_R L_s} \frac{d^2 u_s}{dt^2} + (k_{io} - k_{if}) \frac{d^2 i_{pr}}{dt^2}$$
$$+ k_{io} k_{id} \left(1 + \frac{L_f}{K_R} \right) \frac{d^3 i_{pr}}{dt^3} + k_M \frac{d^2}{dt^2} (u_n u_{ref}). \tag{15}$$

The right-hand side of the equation contains ingredients linked to extortion, which could include also – because of the relatively large time constants of u_{DC} voltage control loop – $u_{n*} u_{ref}$ product of a derivative. In order to analyze the conditions for stability of the system we can consider the free differential equation under the additional assumption of $C_f = 0$. C_f capacitance in the filters of three-level inverter is very small and is designed for filtering of high frequency component generated by the inverter. Omission of the capacity C_f in further discussion is justified by of acute inequality $X_{Ls} + X_{Ll} \ll X_{Cf}$, which holds for the expected frequency of oscillations in unstable operation states, almost equal to the resonant frequency $f_{p,res}$ of $L_p C_p$ passive filter. In [3, 9] this capacity for analysis of active filter operation was omitted.

$$\frac{d^4 i_p}{dt^4}$$
$$+ \frac{K_R \left(k_{up} - \frac{k_{io} k_{id}}{L_p} \right) + 1 + \frac{L_f}{L_s} + \frac{L_f}{L_p}}{k_{ud} K_R} \frac{d^3 i_p}{dt^3}$$
$$+ \frac{k_{if} \left(1 + \frac{L_p}{L_s} \right) - k_{io} + \frac{k_{ud}}{C_p}}{k_{ud} L_p} \frac{d^2 i_p}{dt^2}$$
$$+ \frac{k_{up} K_R + 1 + \frac{L_f}{L_s}}{k_{ud} K_R C_p L_p} \frac{di_p}{dt} + \frac{k_{if}}{k_{ud} C_p L_s L_p} i_p = 0. \tag{16}$$

3. Conditions for stable operation of the circuit

Considering the following labels:

$$a_3 = \frac{k_{up}K_R + 1 - \dfrac{k_{io}k_{id}K_R}{L_p} + \dfrac{L_f}{L_s} + \dfrac{L_f}{L_p}}{K_R k_{ud}}, \quad (17)$$

$$a_2 = \frac{k_{if}\left(1 + \dfrac{L_p}{L_s}\right) - k_{io} + \dfrac{k_{ud}}{C_p}}{L_p k_{ud}} \quad (18)$$

$$a_1 = \frac{k_{up}K_R + 1 + \dfrac{L_f}{L_s}}{K_R C_p L_p k_{ud}}, \quad (19)$$

$$a_0 = \frac{k_{if}}{C_p L_s L_p k_{ud}}, \quad (20)$$

Eq. (16) may be written in its canonic form:

$$\frac{d^4 i_p}{dt^4} + a_3 \frac{d^3 i_p}{dt^3} + a_2 \frac{d^2 i_p}{dt^2} + a_1 \frac{di_p}{dt} + a_0 i_p = 0. \quad (21)$$

4. Criteria for optimizing the control circuit

The specific equation for the differentiation equation show above is:

$$s^4 + a_3 s^3 + a_2 s^2 + a_1 s + a_0 = 0. \quad (22)$$

According to [10] if the specific equation (22) has a multiple root, the transient component waveforms in the control system are aperiodically critical. This condition also means zero value of oscilatibility of the control system (zero overshot of the transient component). According to [11], the shortest recovery time for a given geometric average of real roots occurs when the characteristic Eq. (22) has one multiple root.

Let us assume that Eq. (22) has one real quadruple root s_o. We can then write:

$$s^4 + a_3 s^3 + a_2 s^2 + a_1 s + a_0 = (s - s_o)^4. \quad (23)$$

After bringing the right side of the equation into a polynomial form and comparing the corresponding coefficients of the left and right sides of equations, we obtain the dependencies, fulfillment of which ensures the existence of a single quad root:

$$a_0 = \frac{a_2^2}{36}, \quad (24)$$

$$a_2 = \frac{3}{8}a_3^2, \quad (25)$$

$$a_1 = \frac{a_3^3}{16}. \quad (26)$$

If we assume the following label

$$a_o = \omega_o^4, \quad (27)$$

whereby ω_o means own system vibration pulsation, then we can write the specific equation in a new form:

$$s^4 + 4\omega_o s^3 + 6\omega_o^2 s^2 + 4\omega_o^3 s + \omega_o^4 = 0. \quad (28)$$

The determined coefficients in the specific equation ensure that there is a quadruple real root, which ensures the stability

criterion of aperiodic control system. Table 1 gives the optimal polynomials of different orders ($n = 2, 3, 4, 5$) to ensure fulfillment of this criterion, and to compare polynomials [12] to ensure the minimization of ITAE integral criterion ("the integrity of time multiplied by the value absolute of error"). The transient behavior in a system fulfilling ITAE are characterized by considerably shorter regulation time but with high overshot value.

Table 1

n	criterion of aperiodic stability	ITAE criterion
2	$s^2 + 2\omega_o s + \omega_o^2$	$s^2 + 1.41\omega_o s + \omega_o^2$
3	$s^3 + 3\omega_o s^2 + 3\omega_o^2 s + \omega_o^3$	$s^3 + 1.75\omega_o s^2 + 2.1\omega_o^2 s + \omega_o^3$
4	$s^4 + 4\omega_o s^3 + 6\omega_o^2 s^2$ $+4\omega_o^3 s + \omega_o^4$	$s^4 + 2.1\omega_o s^3 + 3.4\omega_o^2 s^2$ $+2.7\omega_o^3 s + \omega_o^4$
5	$s^5 + 5\omega_o s^4 + 10\omega_o^2 s^3 +$ $10\omega_o^3 s^2 + 5\omega_o^4 s + \omega_o^5$	$s^5 + 2.8\omega_o s^4 + 5\omega_o^2 s^3 +$ $5.5\omega_o^3 s^2 + 3.4\omega_o^4 s + \omega_o^5$

The parameters describing the behavior of the transient component (recovery time, overshoot) in the system that satisfies the aperiodic stability criterion in the general case are similar to those in the system that satisfies the other integral criterion, given in the literature [12] as IAE ("integral of absolute value of error"). IAE criterion, compared to aperiodic stability criterion, provides greater control with higher oscillations but with less regulation time.

For the ITAE criterion we obtain:

$$a_{0,ITAE} = \frac{a_{2,ITAE}^2}{11.56}, \quad (29)$$

$$a_{2,ITAE} = 0.77 a_{3,ITAE}^2, \quad (30)$$

$$a_{1,ITAE} = \frac{a_{3,ITAE}^3}{3.43}. \quad (31)$$

Coefficients k_{ud}, k_{up}, and k_{id} will be determined with the following assumptions:

$$k_{io} = k_{if} = k_i. \quad (32)$$

With the condition (24) or (29) we obtain two solutions describing the k_{ud} coefficient as function of a_o, a_2 (or $a_{o,ITAE}$, $a_{2,ITAE}$) coefficients:

$$k_{ud1,2} = \left(\frac{a_2^2}{2a_o} - 1 \pm 0.5\sqrt{\frac{a_2^2}{a_o}\left(\frac{a_2^2}{a_o} - 4\right)}\right) k_i \frac{L_p C_p}{L_s}, \quad (33)$$

$$k_{ud1} = 33,97 k_i \frac{L_p C_p}{L_s}. \quad (34)$$

From studies of experimental and simulation studies it stems that the values of k_{ud1} calculated according to (34) in practical terms, due to the distortion of the network from other receivers, are too large and are hardly acceptable [2].

For further discussion k_{ud2} coefficient is adopted marked as k_{ud}. If we make mark:

$$\lambda = \frac{a_2^2}{2a_o} - 0.5\sqrt{\frac{a_2^2}{a_o}\left(\frac{a_2^2}{a_o} - 4\right)} - 1. \quad (35)$$

The we can write (33) as:

$$k_{ud} = \lambda k_i \frac{L_p C_p}{L_s}. \quad (36)$$

From conditions (25), (26) or analogous (30), (31) and taking (35), (36) into account we obtain relations describing k_{up} and k_{id}:

$$k_{up} = \sigma \frac{k_i \sqrt{L_p C_p}}{L_s} - \frac{1 + \dfrac{L_f}{L_s}}{K_R}, \qquad (37)$$

where

$$\sigma = \frac{\left(\sqrt{\dfrac{a_3^2}{a_2}(1+\lambda)\lambda} \right)^3}{\dfrac{a_3^3}{a_1}\lambda^2} \qquad (38)$$

and

$$k_{id} = -\gamma \frac{L_p}{L_s}\sqrt{L_p C_p} + \frac{L_p}{k_i K_R}\left(1 + \frac{L_f}{L_s} + \frac{L_f}{L_p}\right) + \frac{k_{up} L_p}{k_i}, \qquad (39)$$

where

$$\gamma = \sqrt[3]{\frac{a_3^3}{a_1}\lambda^2 \sigma}. \qquad (40)$$

Table 2 lists λ, σ, γ coefficients for aperiodic stability and ITAE criterions.

Table 2

	λ	σ	γ
aperiodic stability	0.0294	1.657	0.284
ITAE	0.1	1.574	0.378

For $u_{DC} = 1100$ V, $L_p = 180$ μH, $C_p = 500$ μF, $C_f = 40$ μF, $L_f = 160$ μH, $L_l = 0$ μH, $U_T = 4.9$ V, $f_{syn} = 30$ kHz, $t_{dead} = 2$ us, $K_r = 8.6$ V/V ($K_R = 908$ V/V), $k_i = 0.005$ V/A, we obtain values of k_{up}, k_{ud} and k_{id} listed in Table 3.

Table 3

	L_s [μH]	k_{ud} [s]	k_{up} [V/V]	k_{id} [s]
aperiodic stability	100	$1.3 \cdot 10^{-7}$	0.022	$8 \cdot 10^{-4}$
	200	$0.64 \cdot 10^{-7}$	0.011	$4 \cdot 10^{-4}$
ITAE	100	$4.4 \cdot 10^{-7}$	0.021	$7 \cdot 10^{-4}$
	200	$2.2 \cdot 10^{-7}$	0.0097	$4 \cdot 10^{-4}$

Values of k_{ud}, k_{up} and k_{id} were determined in accordance with the criterion of aperiodic stability , for which k_{ud} undoubtedly obtains a lower value compared to the value determined for ITAE. Voltage derivative signal sent to the current controller input for large deformation of the mains voltage has a negative impact on the quality of filtration. The quality of filtration can be improved by substituting the signal proportional to the derivative of the corresponding phase load current for the signal proporional to the derivative of the passive filter current. This is justified by assuming that the 6D rectifier input currents represent 3-phase current source. Under this assumption, equation (16) does not change. However, this solution requires the installation of additional current sensors in the branches of *LpCp* passive filter.

5. Simulation tests

Simulation tests were performer for $k_{up} = 0.022$, $k_{ud} = 1.3 \cdot 10^{-7}$, $k_{id} = 8 \cdot 10^{-4}$ (or $k_{up} = 0$, $k_{ud} = 0$, $k_{id} = 0$) coefficients determined according to aperiodic stability criterion for $L_s = 100$ μH. For the generation of the current reference, the switches $S1$, $S2$, $S3$ were conducting in Fig. 2. Figures 5 to 8 show waveforms of filter inverter output voltage (u_{f2}), input phase voltage (u_{c23}), the current (i_{pr2}) drawn by the 6D rectifier, current (i_{p2}) drawn by the passive filter and the current (i_{s2}) drawn from the supply grid for the four cases presented in the respective figures:

1° R_o=1.5 Ω, k_{up}=0, k_{ud}=0 and k_{id}=0,
2° R_o=1.5 Ω, k_{up}=0.022, k_{ud}=1.3 $\cdot$ 10^{-7}, k_{id}=8 $\cdot$ 10^{-4},
3° R_o=1.5 kΩ, k_{up}=0, k_{ud}=0, k_{id}=0,
4° R_o=1.5 kΩ, k_{up}=0.022, k_{ud}=1.3 $\cdot$ 10^{-7}, k_{id}=8 $\cdot$ 10^{-4}.

The waveforms shown in figures show that the power supply system with passive filter and active filter regardless of the 6D rectifier load stable operation of the system can be assured by introducing feedbacks defined in article with coefficients given in Table 3.
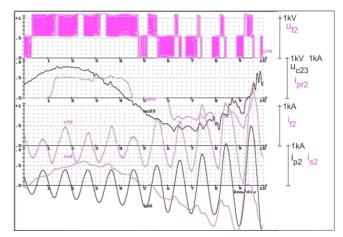

Fig. 5. Waveforms of voltages u_{f2}, u_{c23} (1 kV/div) and currents i_{pr2}, i_{f2}, i_{p2}, i_{s2} (1 kA/div) for $R_o = 1.5$ Ω, $k_{up} = 0$, $k_{ud} = 0$ and $k_{id} = 0$
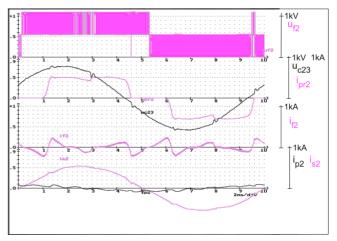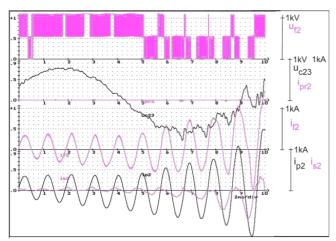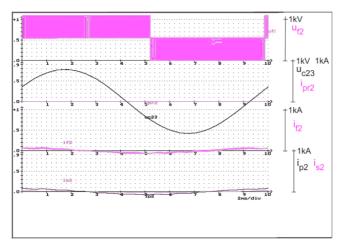

Fig. 6. Waveforms of voltages u_{f2}, u_{c23} (1 kV/div) and currents i_{pr2}, i_{f2}, i_{p2}, i_{s2} (1 kA/div) for $R_o = 1.5$ Ω, $k_{up} = 0.022$, $k_{ud} = 1.3 \cdot 10^{-7}$ and $k_{id} = 8 \cdot 10^{-4}$

Fig. 7. Waveforms of voltages u_{f2}, u_{c23} (1 kV/ div) and currents i_{pr2}, i_{f2}, i_{p2}, i_{s2} (1 kA/div) for $R_o = 1.5$ kΩ, $k_{up} = 0$, $k_{ud} = 0$ and $k_{id} = 0$

Fig. 8. Waveforms of voltages u_{f2}, u_{c23} (1 kV/div) and currents i_{pr2}, i_{f2}, i_{p2}, i_{s2} (1 kA/div) for $R_o = 1.5$ kΩ, $k_{up} = 0.022$, $k_{ud} = 1.3 \cdot 10^{-7}$ and $k_{id} = 8 \cdot 10^{-4}$

u_{f2} voltage is the output voltage of the central branch of multilevel inverter, referring to the negative supply bus of the inverter. Simulation results indicate correct filter operation. Total harmonics voltage distortion in comparison between voltages u_{c23} shown in Fig. 5 and Fig. 6 is reduced from 14.87% to 2.39%. The passive displacement power factor for the case of 6D rectifier load and stable operation of the system is 0.999.

6. Experimental studies

In order to verify the correctness of the algorithm used FAW3-200k-600 active filter produced in MEDCOM company was studied.

The study was conducted for the following parameters: $u_{DC} = 1100$ V, $C_p = 500$ μF, $L_p = 180$ μH, ($f_{p,res} = 531$ Hz), $C_f = 40$ μF, $L_f = 160$ μH, $L_l = 17$ μH, $L_s = 200$ μH, $U_T = 3$ V, $f_{syn} = 20$ kHz, $t_{dead} = 2$ μs, $K_r = 6.8$, ($K_R = 1196$), $k_i = 0.005$, $k_{ud} = 0$, $k_{id} = 0$, $k_{up} = 0.0075$ (or $k_{up} = 0$, $k_{ud} = 0$, $k_{id} = 0$). For the generation of the current reference, the switches $S1$, $S2$, $S3$ were

open in Fig. 2. The tests were performer with resonant L_pC_p branch without any load at the output of 6D converter.

$L_s = 200$ μH inductance corresponds to the total dissipation inductance of the power supply and three-phase transformer with 200 kV output power (400 V/600 V) applied power to the filter and load. Power supply receiver-active filter system through transformer allowed to test the system with a filter having a rated voltage of 3×600 V and reduce the impact of industrial network deformation on the results of the study.

Waveforms examples taken in the system with active filter are shown below. The picture shown in Fig. 9 shows the waveforms of output current of the inverter and the filter output current (upper and middle waveform) and the C_f capacitor current (bottom) in the state of active filter unstable operation, in the absence of feedback from the AC voltage at the terminals of the filter. In a practical system the inverter output current is limited to instantaneous value of 600 A, which results in a current similar to triangular shape.
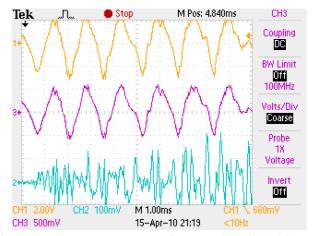

Fig. 9. Inverter output current waveform i_{f2} (CH1:400 A/div), output filter current i_{l2} (CH2:500 A/div), and capacitor C_{f2} current i_{cf2} (CH3:100 A/div) for $k_{up} = 0$, $k_{ud} = 0$, $k_{id} = 0$

The waveform shown in Fig. 10 shows the inverter output current i_{f2} for $k_{up} = 0.0075$, $k_{ud} = 0$ and $k_{id} = 0$.
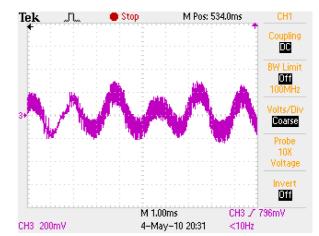

Fig. 10. Inverter output current waveform i_{f2} (CH3:40 A/div) for $k_{up} = 0.0075$, $k_{ud} = 0$, $k_{id} = 0$

The stability of the system was obtained by introducing to the controller input only a signal proportional to the voltage measured at the terminals on the AC side of the inverter. Although, this means lack of aperiodic stability criterion, but allows to avoid the potential distortions introduced by differentiating systems. In order to investigate the negative impact of introduced feedback from the AC voltage on the quality of filtration additional experiments were carried out with a passive filter is off, whose results are shown in Figs. 11 and 12. The active filter worked with voltage feedback coefficient $k_{up} = 0.0075$.
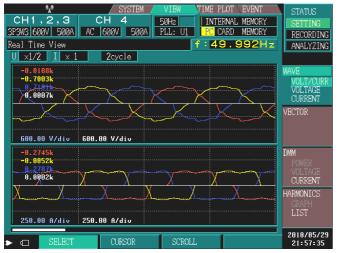

Fig. 11. Waveforms of phase input grid voltages (upper figures 600 V/div) and currents drawn from the grid (lower figures 250 A/div) for system without the filter
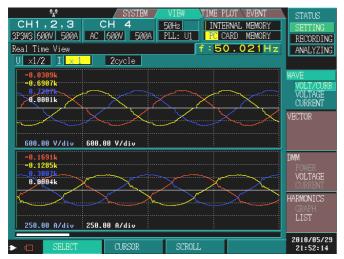

Fig. 12. Waveforms of phase input grid voltages (upper figures 600 V/div) and currents drawn from the grid (lower figures 250 A/div) for system with the filter on

The filter reduced the level of distortion of the supply current THD_i of the value of 24.5% to 5.72% and voltage distortion from 9.49% to 3.60%.

The results of the FA3-200K-600 filter presented in this article are in addition to the results described in [13].

7. Conclusions

The results of simulation and experimental studies show that for the power system in which the active filter compensates the distortion power introduced both by a non-linear load and a displacement reactive power introduced by a serial resonant circuit passive filter, the stability of the system can be ensured by a feedback from the AC voltage. In a practical system, bringing the signal proportional to the voltage provided a stable operation of the filter.

According to a study presented in [2], in the case of a purely capacitive load, the weight derivative of AC voltage is dominant.

Taking into account the conclusions of [2] and the results presented in this paper it can be stated that the signal proportional to the AC mains voltage and the derivative of this signal provides – for the described control algorithm – stable operation of an active filter in the system with capacitive load maintaining good dynamic parameters with regard to the reproduction of sinusoidal shape of the supply current at a sudden change of active power consumed by the receiver.

However, compliance with the assumption that the solution of the characteristic equation is a quadruple real root, requires the introduction of the three signals to the control system. The analysis and testing of both simulation and experimental, selected results which are presented in the article, it follows that the values of the coefficients set by Eqs. (36), (37) and (39) ensure the stable operation of the active filter, used as a compensator of deformation power and/or displacement capacitive reactive power contributed by the serial resonant LC circuit of a passive filter with a total power equal to the rated filter power.

REFERENCES

[1] G. Benysek, M.P. Kazmierkowski, J. Popczyk, and R. Strzelecki, "Power electronic systems as a crucial part of smart grid infrastructure – survey", *Bul. Pol. Ac.: Tech.* 58 (4), 455–473 (2011).

[2] T. Platek, "Power system stability with parallel active filter ensuring compensation of capacitive reactive power", *Electrical Review* 12a, 173–177 (2011).

[3] X. You, Y. Li, R. Hao, and Z. Cheng, "A new synchronous frame current reference generation for hybrid active filter and system stability analysis", *Proc., IECON'03: 29th Annual Conf. IEEE* 3, 2011–2016 (2003).

[4] M. Paolo, "A closed-loop selective harmonic compensation for active filters", *IEEE Trans. on Industry Applications* 37 (1), 81–89 (2001).

[5] P. Brogan and R. Yacamini, "Stability of selective harmonic active filters", *Proc. 8th Int. Conf. Power Electronics Variable Speed Drivers* 1, 416–421 (2000).

[6] M. Bobrowska-Rafal, K. Rafal, M. Jasinski, and M.P. Kazmierkowski, "Grid synchronization and symmetrical components extraction with PLL algorithm for grid connected power electronic converters – a review", *Bul. Pol. Ac.: Tech.* 58 (4), 485–497 (2011).

[7] H. Akagi, E.H. Watanab, and M. Aredes, *Instantaneous Power Theory and Applications to Power Conditioning*, IEEE Press, Willey-Interscience, London, 2007.

[8] T. Platek and J. Rabkowski, "Modulator of FLC three-level inverter with flying capacitor voltage balancing", *Electrical Review* 4, 266–272 (2010).

[9] M. Machmoum, N. Bruyant, S. Siala, and R.A. Le Doeuff, *Practical Approach to Harmonic Current Compensation by a Single-Phase Active Filter*, Epe, Sevilla, 1995.

[10] Z. Jędrzykiewicz and Ł. Węsierski, "Theory of control and automation. Part I", *University Scripts AGH* 682, CD-ROM (1979).

[11] T. Kaczorek, *Control Theory, Linear and Discrete Systems*, PWN, Warsaw, 1997.

[12] F. Zach, *Technisches Optimieren*, Springer Verlag, Wien, 1974.

[13] T. Platek, T. Osypinski, and J. Rabkowski, "Active filter for power engineering with three level FLC inverter and high rate of rise of compensation current", *Electrotechnical News* 9, 65–68 (2010).